

Optimal boundary control of a contact thawing process for foodstuff

Christoph Josef Backi ^{*,1} John Leth ^{**} Jan Tommy Gravdahl ^{***}

^{*} Department of Chemical Engineering, Norwegian University of Science and Technology, N-7491 Trondheim, Norway (e-mail: christoph.backi@ntnu.no).

^{**} Department of Electronic Systems, Aalborg University, DK-7220, Aalborg, Denmark (e-mail: jjl@es.aau.dk)

^{***} Department of Engineering Cybernetics, Norwegian University of Science and Technology, N-7491 Trondheim, Norway (e-mail: jan.tommy.gravdahl@ntnu.no).

Abstract: In this work an approach for thawing blocks of foodstuff, in particular fish, is introduced. The functional principle is based on plate freezer technology, which has been used in industry for decades. The aim of this work is to describe the temperature dynamics of this thawing process by means of partial differential equations (PDEs) and control the boundary conditions in an optimal way. The PDE describing the temperature dynamics is based on the diffusion equation with state-dependent parameter functions.

Keywords: Thawing, Foodstuff, Partial Differential Equations, Optimal Control, MPC

1. INTRODUCTION

Shelf life extension of rapidly spoiling foodstuff is an essential task for the food industry. This holds especially for fish and fish products as they often have to be transported over long distances or stored over long periods in order to deliver them to the consumer or to further processing stages. By lowering the temperature, the rate of spoilage is reduced. As a general rule it holds that, the lower the temperature, the longer the shelf life. Therefore, freezing is the best method for shelf life extension over long periods.

After having been transported over long distances or stored over long periods, the foodstuff might not necessarily be sold in frozen state, but processed further. For example, frozen fillets in block form can be cut more or less directly to fish sticks after a short tempering phase, see Jason (1974). On the other hand, filleting of headed and gutted fish is not possible in frozen state. Therefore, thawing techniques must be used in order to enable further processing. Thus, not only freezing has a large impact on the quality of the final product, but also thawing. Thawing can not enhance the quality of the frozen product, meaning that quality losses and damages caused in earlier stages cannot be reversed by even the most sophisticated way of thawing. Hence it is even more important to understand the process of thawing, come up with new, gentle methods, derive mathematical models and in the end control the process such that an optimal solution is obtained, meaning that quality losses in the thawing process can be minimized.

As quality is influenced by many factors and parameters, a more precise definition for the process of thawing is needed. The most critical quality parameters influenced by the thawing process are water holding capacity, drying of the surface and lipid oxidation. Not only do they lower the overall quality directly, but also the product's yield. Reduced water holding

capacity leads to increased drip loss, which results in lower product weight. Drying of the surface also results in lower product weight, whereas lipid oxidation occurs mostly for fatty species and can cause rancid tastes and smells. Both, drying and lipid oxidation are most likely to happen in air-based thawing methods.

There is a whole range of publications in the scientific community introducing different methods for freezing and thawing of foodstuff, see e.g. Johnston et al. (1994) and Jason (1974). Moreover, the modeling of heat and mass transfer phenomena with PDEs has extensively been studied, e.g. in Pham (2006b) and Pham (2006a). In Cleland et al. (1987) experimental data for freezing and thawing of multi-dimensional objects modeled by finite element techniques are presented. As computational power has grown in recent years, complex simulations can provide qualitative and quantitative insights to the system, even in the absence of analytical solutions. An open-loop approach for optimal boundary control of a plate freezing process has been described in Backi and Gravdahl (2013). However, it must be mentioned that thawing is not simply the reversed freezing process, as for example outlined in Olver (2014, Section 4.1). There it is mentioned that the *backwards heat equation*, where future and past are changed by changing from t to $-t$, is an ill-posed problem in the sense that small changes in initial data can lead to randomly large changes in the solution arbitrarily close to initial time.

Applied methods for thawing of fish blocks in industry are mostly based on heat conduction and convection by direct contact with the thawing medium. For this purpose mostly water or air are used. In water-based techniques the fish blocks are put into a water bath. Added air bubbles enhance heat transfer. In addition the water is sometimes heated in order to speed up the process. Another method relies on heat transfer by moving air, known as air-blast thawing. Due to the danger of lipid oxidation and drying of the surface it should be conducted with

¹ corresponding author

humidified air. The two mentioned methods are only controllable to a small extent as the physical processes underlying heat transfer are complex. The mentioned disadvantages motivate the introduction of another thawing method that is not as widely spread in industry as the two mentioned before. It does not rely on heat transfer by direct contact with the thawing medium, but on principles already known from plate freezer technology. Hereby a refrigerant flows through the plate freezer walls, where it vaporizes and extracts heat from the fish block. The thawing approach investigated here relies on the same principle, but instead of using a refrigerant, a thawing medium with high specific heat capacity can be used to thaw the fish block. The thawing medium, however, does not undergo phase change during the process.

To the authors best knowledge no work has been done so far in modeling the temperature dynamics of a contact thawing process. Also the important matter of (optimal) control of such a process has not been covered. Therefore this work presents a novelty with respect to the field of application.

The rest of the paper is organized as follows. Section 2 introduces the model and addresses some issues regarding the application of this model to both, freezing and thawing processes. Section 3 describes the problem setting for Model Predictive Control, whereas Section 4 shows numerical simulation examples that highlight the results in the previous section. Finally, Section 5 provides some concluding remarks.

2. PROBLEM FORMULATION

The process of thawing foodstuff is often performed based on thermodynamic steady state calculations (prior to execution), meaning that the temperature dynamics are neglected. In order to obtain better monitoring and in the end control the quality during thawing, the temperature dynamics play a vital role. However, these temperature dynamics and the temperature distribution throughout the foodstuff are hard to model in standard ways of thawing, such as immersion or air-blast processes. Thus we propose a contact thawing process in order to monitor and control the foodstuff's interior temperature field, which directly influences the quality. The choice of contact thawing is justified by the fact that the related process of freezing in plate freezers is well-understood and its results in modeling can be directly applied to the contact thawing process. Existing monitoring-algorithms to estimate the temperature field inside the foodstuff can be adapted to the contact thawing application, see e.g. Backi et al. (2015).

The overall aim of this work is to provide an optimal boundary control formulation for a contact thawing process such that determined temperature margins can be satisfied during the whole operation. This is beneficial for the final product quality.

It must be mentioned here that the time it takes to thaw foodstuff is significantly larger than to freeze it. The reason for this is that ice is a better conductor of heat compared to water. This means that for freezing the heat flow from the inner domain towards the boundary layer is accelerated over time due to ice layer formation at the boundary propagating towards the interior. For thawing, however, an initial liquid layer builds up at the boundary and propagates towards the interior causing a decrease in heat flow from the boundary to the inside of the food over time.

2.1 System structure

In Figure 1 we propose a control structure for the thawing process consisting of a cold water feed, a hot water buffer tank, two pumps and three (controlled) valves. The idea is to use an algorithm based upon Model Predictive Control (MPC) controlling the unit consisting of the two pumps and the valve mixing the hot and the cold water such that the desired boundary temperature in the thawer can be adjusted. The return water from the thawer can be split up to be either fed back to the hot water buffer tank or be disposed via the outlet (parts of it could also be fed back to the cold water feed, for example).

In the present work only the temperature dynamics of the thawer will be considered. In addition, we assume that the required temperature of the thawing medium can be exactly provided by the valve combining the hot and cold water feed. It is explicitly not intended to provide an underlying control structure for the unit providing the desired water (and thus boundary) temperature to the thawer. This is a task for future work and can result in energy-efficient operation.

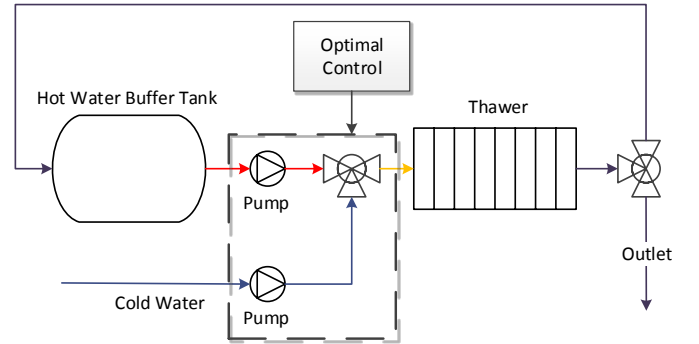


Fig. 1. Functional principle of the contact thawing process

2.2 Temperature dynamics model in the thawer

To model the temperature dynamics of the food in the thawer we use the diffusion equation with state-dependent parameters in the variable $T = T(t, x)$, which can be expressed in the following standard form:

$$\rho(T) c(T) T_t = [\lambda(T) T_x]_x \quad (1)$$

subject to (controlled) Dirichlet boundary conditions

$$T(t, 0) = T(t, L) = u, \quad (2)$$

where $\rho(T) > 0$ denotes the density, $c(T) > 0$ indicates the specific heat capacity and $\lambda(T) > 0$ describes the thermal conductivity of the good inside the thawer. Note that $\rho(T)$, $c(T)$ and $\lambda(T)$ all depend on the temperature T . For completeness we point out that u is the control variable (input), whereas its derivative $\dot{u} = v$ is the optimization variable, see Section 3.2.

The diffusion equation (1) can be rewritten as

$$\rho(T) c(T) T_t = \lambda_T(T) T_x^2 + \lambda(T) T_{xx}. \quad (3)$$

due to

$$\lambda_x(T) = \lambda_T(T) T_x.$$

To keep notation simple, two new parameters can be introduced as

$$k(T) = \frac{\lambda(T)}{\rho(T)c(T)}, \quad (4)$$

$$\kappa(T) = \frac{\lambda_T(T)}{\rho(T)c(T)},$$

leading to a rewritten form of (3):

$$T_t = \kappa(T) T_x^2 + k(T) T_{xx}. \quad (5)$$

For freezing, (5) has extensively been studied, for example in Backi et al. (2015), where a stability investigation as well as an observer design have been conducted, and in Backi et al. (2014), where in addition similarities to the (potential) Burgers' equation were presented.

2.3 Parameters

The model (5) does not explicitly model the physical behaviour at and around the freezing point T_F . The presence of *latent heat of fusion* causes so called *thermal arrest*, which means that the temperature around the freezing point remains constant until the specific amount of *latent heat of fusion* is removed from (in the freezing case) or added to (in the thawing case) the object. One approach to model this phenomenon is to *overestimate* $c(T)$ in a region around the freezing point $I_{\Delta T} = T_F \pm \Delta T$, such that heat conduction is lowered in this region. This method is called *apparent heat capacity method* and has been described generally in e.g. Muhieddine et al. (2008). Figure 2 displays a qualitative sketch of the parameters $\lambda(T)$ and $c(T)$ over T . We remark that the temperature dependence of $\rho(T)$ is insignificant compared to $\lambda(T)$ and $c(T)$ and therefore approximated as $\rho(T) = 950 \text{ kg m}^{-3} = \text{const.}$

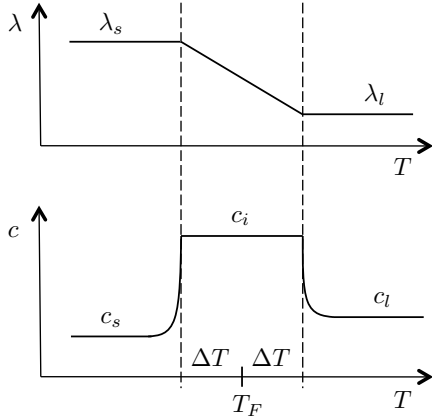


Fig. 2. Qualitative sketch of parameters λ and c over T

Parameter functions based on real experimental data defining $c(T)$ and $\lambda(T)$ as thermodynamic alloys of different substances such as water, fat, carbohydrates, etc. are described in Harðarson (1996) resulting in $[\lambda_s \lambda_l] = [1.8 \ 0.5] \text{ W m}^{-1}\text{K}^{-1}$ and $[c_s \ c_i \ c_l] = [2200 \ 283000 \ 3800] \text{ J kg}^{-1}\text{K}^{-1}$.

In Figures 3 and 4 the blue plots represent the parameter functions $k(T)$ and $\kappa(T)$ calculated with (4) and the definitions in Figure 2 whereas in red the approximations of $k(T)$ and $\kappa(T)$ based on arctan-expressions are shown. These arctan-functions are displayed in Appendix A and are used in the optimization software package ACADO (see Section 4). As can be seen from Figure 3, the overestimation of $c(T)$ in the region $T_F \pm \Delta T$, with

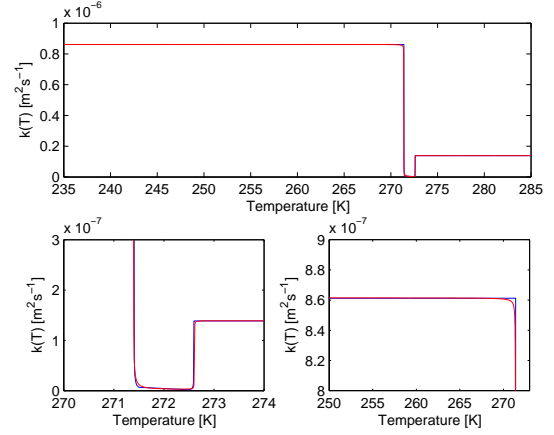


Fig. 3. $k(T)$, based on piecewise constant definitions of $c(T)$ and $\lambda(T)$ (blue) and approximated by arctan-expressions (red), the two bottom plots represents zooms into a specific temperature region

$T_F = 272 \text{ K}$ and $\Delta T = 0.5 \text{ K}$ causes a significant decrease of the thermal diffusivity $k(T)$ in that region.

Figure 4 presents the parameter function $\kappa(T)$, which is only nonzero inside $T_F \pm \Delta T$ for the piecewise continuous definitions of $\lambda(T)$ and $c(T)$. For the arctan-approximation the values are nonzero also outside $T_F \pm \Delta T$, however, very small.

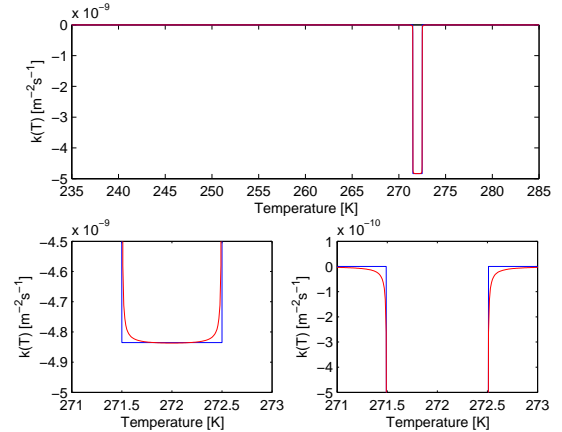


Fig. 4. $\kappa(T)$, based on piecewise constant definitions of $c(T)$ and $\lambda(T)$ (blue) and approximated by arctan-expressions (red), the two bottom plots represents zooms into a specific temperature region

3. MODEL PREDICTIVE CONTROL

We are going to optimally control the temperature distribution inside the block of foodstuff during thawing by using an MPC algorithm. Therefore it will be necessary to discretize the PDE. Both, discretization in space and time are possible, however, as we are going to design a continuous MPC scheme, the discretization will only be performed for the spatial domain.

3.1 Discretization

As outlined above, the model (5) is discretized in the spatial domain only, a so-called semi-discretization approach. This

leads to a set of continuous, coupled (interdependent) ODEs. Forward, backward and central difference schemes are used in order to discretize the term T_x , whereas only central differences are applied for the term T_{xx} . The overall scheme holds for $n = 1, 2, \dots, N$, with N odd, and can be seen in the following

$$T_x = \begin{cases} \frac{T_{n+1} - T_n}{\Delta x}, & \text{if } n \in R_L = \{1, 2, \dots, \frac{N-1}{2}\} \\ \frac{T_{n+1} - T_{n-1}}{2\Delta x}, & \text{if } n = R_M = \frac{N+1}{2} \\ \frac{T_{n-1} - T_n}{\Delta x}, & \text{if } n \in R_R = \{\frac{N+3}{2}, \frac{N+5}{2}, \dots, N\}, \end{cases} \quad (6)$$

$$T_{xx} = \frac{T_{n+1} - 2T_n + T_{n-1}}{\Delta x^2},$$

The fictional states (*ghost cells*) at T_0 and T_{N+1} represent the boundary conditions (inputs; control variables) and enter the equations exclusively in the discretization of the second order partial derivative with respect to the state variable.

Discretizing (5) using (6) ultimately leads to a set of interdependent, nonlinear ODEs:

$$\dot{T}_n = \begin{cases} \kappa(T_n) \frac{(T_{n+1} - T_n)^2}{\Delta x^2} + k(T_n) \frac{T_{n+1} - 2T_n + T_{n-1}}{\Delta x^2}, & n \in R_L \\ \kappa(T_n) \frac{(T_{n+1} - T_{n-1})^2}{4\Delta x^2} + k(T_n) \frac{T_{n+1} - 2T_n + T_{n-1}}{\Delta x^2}, & n = R_M \\ \kappa(T_n) \frac{(T_{n-1} - T_n)^2}{\Delta x^2} + k(T_n) \frac{T_{n+1} - 2T_n + T_{n-1}}{\Delta x^2}, & n \in R_R, \end{cases} \quad (7)$$

It is clear that for large numbers of discretization steps the results will converge towards the “real” (analytical) solution of (5). In this work, however, the spatial discretization is chosen as $N = 25$ discretization steps. This is due to reduced computational complexity as the MPC algorithm is supposed to deliver its results in real-time. Nevertheless, we point to Backi (2015, Appendix A.2), where a comparative investigation between different discretization resolutions using the scheme in (6) and the commercial MATLAB[®] solver `pdepe` is presented. This investigation leads to the conclusion that a resolution of $N = 25$ covers the dynamics sufficiently well for the present application.

3.2 Algorithm

The MPC consists of a cost function incorporating reference tracking for states, the rate of temperature change at the boundaries (optimization variable) and the temperature at the boundaries (control variable; input), respectively. In addition, we are going to introduce constraints to the system. We require the temperature at the boundaries to be in the band 283 K – 293 K, as temperatures below this band cause a too small driving force for heat exchange and temperatures above this band will lead to quality degradation (caused by protein denaturation). Furthermore, the temperature rate of change v is limited to 1 K per 100 s to account for the dynamics of the supplying components displayed in Figure 1.

Hence, the cost functions looks as follows

$$\min_v J = \int_0^\tau (T - T_{ref})^T Q (T - T_{ref}) + R(u - u_{ref})^2 + S(v - v_{ref})^2 dt$$

subject to

$$\begin{aligned} \dot{T} - f(T, u) &= 0, \\ \dot{u} &= v \\ T(0) &= T_{init}, \\ u(0) &= u_{init}, \\ T &\leq \bar{T}, \\ \underline{v} \leq v &\leq \bar{v}, \\ \underline{u} \leq u &\leq \bar{u}, \end{aligned}$$

where $\dot{T} - f(T, u) = 0$ denotes the set of interdependent ODEs (7) and $\dot{u} = v$ indicates that the optimization variable v is the rate of change of the boundary temperature u . The remaining five equations indicate initial values for the temperatures (T_{init}) and the boundary temperatures (u_{init}) as well as an upper bound for the temperatures (\bar{T}) and lower and upper bounds for the rate of change of the boundary temperature (\underline{v} and \bar{v}) and the boundary temperature itself (\underline{u} and \bar{u}). The positive definite matrix Q has only nonzero entries on the diagonal, whereas R and S are scalars. All numerical values are collected in the table in the Appendix.

The nature of the thawer dictates that at first the outer layers of the block are heated up before the warm front propagates to the center of the spatial domain. Thus the reference temperature T_{ref} in the objective function gets chosen such that the reference values are increasing from the middle towards the outer layers. In the very center the reference temperature is chosen to be 272.5 K, which is just outside the latent zone, meaning that the block is fully thawed. The reference for the boundary temperature u is defined as 283 K, which is assumed to be the thawing medium’s initial temperature and the temperature of the cold water feed. This shall account for saving energy as less water will have to be drained from the hot water buffer tank. The reference for the rate of change of the boundary temperature, v , is set to 0 K s⁻¹ as a steady boundary temperature is desired.

3.3 Stability of the MPC scheme

Stability of the MPC algorithm is an important property and can be enforced for example by introducing so called *terminal region constraints* and/or *terminal penalty terms* (also for nonlinear MPC). This can be achieved by quasi-infinite horizon nonlinear MPC schemes, where the terminal region and the terminal penalty term are calculated off-line. The aim is to find an upper approximation for the infinite horizon cost functional, which itself guarantees stability, as described for example in Findeisen and Allgöwer (2002). These stability results hold for systems, whose steady state is the origin.

The steady state for model (5), however, is dictated by the boundary conditions, as it is known that the steady state will converge to a straight line between the boundary conditions (Backi et al. (2015)). This means that with every change of the boundary temperature, different steady state values will be defined. To implement this into an MPC scheme seems impractical for the present case and therefore the system will not be transformed to have the origin as equilibrium point. However, it must be mentioned that there exist methods to handle stability enforcing MPC schemes for families of setpoints, as introduced in Findeisen and Allgöwer (2000). These methods are based upon pseudolinearization of the nonlinear system dynamics, which can be done off-line. This, however, has the disadvantage of being computationally excessive.

The fact that the present case is a batch process, where a tracking rather than a classical stabilization problem has to be solved (the reference values explicitly differ from the steady state values), and that, in addition, the system dynamics are stable (bounded) for bounded inputs, makes a stability investigation unnecessary.

4. SOLVING STRATEGY AND SIMULATION RESULTS

Simulations have been conducted with the Optimization package ACADO for Matlab, see e.g. Houska et al. (2011) and Ariens et al. (2010). In order to use ACADO, the parameter functions $k(T)$ and $\kappa(T)$ have to be defined as continuous functions. The approximations based on arctan-expressions and the simulation parameters can be found in the Appendix.

4.1 Solution strategy for the optimization problem

The optimization problem is solved by a direct single shooting method. This represents a sequential approach, for which the time horizon τ gets divided into a fixed time grid $0 = t_0 < t_1 < \dots < t_G = \tau$. This time grid does not necessarily have to be equidistant, however, due to convenience it is chosen as such. Nevertheless, it should be pointed out that some problems might be solved more efficiently and faster if the time grid is defined non-equidistant. Between each of these time instances a piecewise constant input function, the optimization variable, gets chosen and implemented into the ODEs. However, piecewise constant input functions are often not practical due to their stepwise definition. Therefore, as mentioned before, the rate of change of the boundary temperature v is chosen as the optimization variable, which, after integration, will result in a continuous boundary temperature u , which is inserted into (7).

Discretizing the optimization and respectively the control variable (input) in the aforementioned fashion and insertion into the objective value and constraints defines a Nonlinear Programming (NLP) problem. An NLP can be solved by different methods (e.g. Interior point methods), however, Sequential Quadratic Programming (SQP), an iterative method, is often the most effective for shooting methods as they generate small and dense NLPs. This is done by defining quadratic (QP) optimization subproblems, which are solved by an active-set strategy relying on linearized dynamics and constraints. Here, line search algorithms are used in order to find a search direction leading to a decrease in the objective function. Thus, one SQP iteration delivers an optimal search direction, however, this may have been achieved by several iterations solving the QP. The integration method used to solve the QP is a Runge Kutta method of order 7/8 with relative tolerance 10^{-6} . The built-in QP solver in ACADO is *qpOASES*, an open-source C++ implementation of an active set strategy. The Hessian is chosen to be an approximation of Gauss-Newton type and the tolerance level for the *Karush-Kuhn-Tucker* conditions is set to 10^{-6} .

The time horizon is set to $\tau = 500$ s, where 5 equidistant time-steps are chosen, and hence $\Delta\tau = 100$ s. The first time sequence of 100 s is used as an input to the plant. This represents a trade-off between numerical accuracy and computational speed. After each MPC iteration the states obtained by simulation get perturbed by white Gaussian noise with power = 0.01 dBW before being fed back as new initial conditions to the optimizer. This shall model for both measurement and modeling errors, leading to an application, which is closer to the real world

and rendering the initially symmetric problem non-symmetric. The initial conditions are typically estimated; Observer designs related to these classes of problems are introduced in e.g. Backi et al. (2015) and Backi (2015). The simulation is terminated when all states are larger than 272.5 K, meaning that all states are above the latent zone $I_{\Delta T}$.

4.2 Simulation results

Figure 5 shows the optimization variable (rate of change of the boundary temperature) together with its constraints in red, whereas the control variable (boundary temperature) itself and the respective constraints in red can be seen in Figure 6. It must be pointed out that actuation is only needed in roughly the first 4000 s with the chosen simulation parameters.

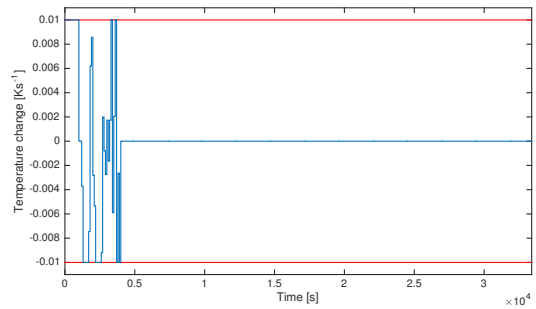


Fig. 5. Rate of change v of the boundary temperature over time

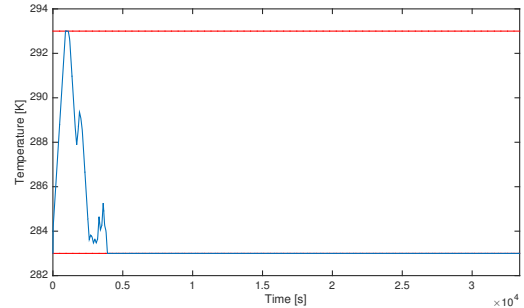


Fig. 6. Boundary temperature u over time

In Figure 7 specific temperatures over time are shown. Note that the temperatures for e.g. $n = 1$ and $n = 25$ are not identical due to the perturbation with white Gaussian noise.

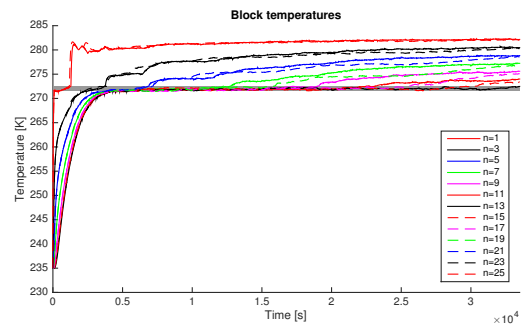


Fig. 7. Specific temperatures over time

In Figure 8, temperatures at the end of the simulation time are visualized in blue together with the reference temperatures T_{ref} in red.

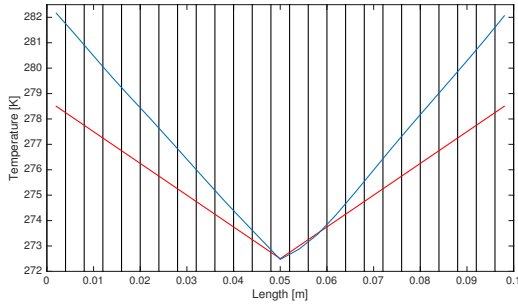


Fig. 8. Temperatures at the end of simulation (blue) and T_{ref} (red)

5. CONCLUSION

In this paper a method for thawing blocks of foodstuff in a contact thawing device was introduced. In addition, a functional principle for such a contact thawing device was proposed. Furthermore, a mathematical model for thawing processes based on the diffusion equation with state-dependent parameters was defined.

In a simulation study, Model Predictive Control (MPC) was used in order to find an optimal solution for controlling the temperature field inside the block of foodstuff in the thawer. The simulation examples presented in Section 4 illustrate that the control objectives could be achieved. The constraints were satisfied even in the presence of added white Gaussian noise, which represents measurement noise and modeling errors.

REFERENCES

- Ariens, D., Ferreau, H.J., Houska, B., and Logist, F. (2010). *ACADO for Matlab User's Manual*. Optimization in Engineering Center (OPTEC) and Department of Electrical Engineering, K. U. Leuven, Leuven, Belgium, Version 1.0beta - v2022 edition.
- Backi, C.J., Bendtsen, J.D., Leth, J., and Gravdahl, J.T. (2014). The nonlinear heat equation with state-dependent parameters and its connection to the Burgers' and the potential Burgers' equation. In *Proceedings of the 19th IFAC World Congress*. Cape Town, South Africa.
- Backi, C.J., Bendtsen, J.D., Leth, J., and Gravdahl, J.T. (2015). A heat equation for freezing processes with phase change: Stability analysis and applications. *International Journal of Control*, 89(4), 833–849.
- Backi, C.J. and Gravdahl, J.T. (2013). Optimal boundary control for the heat equation with application to freezing with phase change. In *Proceedings of the 3rd Australian Control Conference*. Perth, Australia.
- Backi, C.J. (2015). *Modeling, Estimation and Control of Freezing and Thawing Processes - Theory and Applications*. Ph.D. thesis, Norwegian University of Science and Technology, Trondheim, Norway.
- Cleland, D.J., Cleland, A.C., Earle, R.L., and Byrne, S.J. (1987). Experimental data for freezing and thawing of multi-dimensional objects. *International Journal of Refrigeration*, 10, 22–31.

- Findeisen, R. and Allgöwer, F. (2000). A Nonlinear Model Predictive Control Scheme for the Stabilization of Setpoint Families. *Journal A, Benelux Quarterly Journal on Automatic Control*, 1(41), 37–45.
- Findeisen, R. and Allgöwer, F. (2002). An Introduction to Nonlinear Model Predictive Control. In *Proceedings of the 21st Benelux Meeting on Systems and Control*, 119–141. Veldhoven, The Netherlands.
- Harðarson, V. (1996). *Matvarens termofysiske egenskaper og deres betydning ved dimensjonering av frysetunneler*. Ph.D. thesis, Universitetet i Trondheim – Norges Tekniske Høgskole.
- Houska, B., Ferreau, H.J., and Diehl, M. (2011). ACADO Toolkit - an open-source framework for automatic control and dynamic optimization. *Optimal Control Applications and Methods*, 32, 298–312.
- Jason, A.C. (1974). *Thawing Frozen Fish*. Torry Advisory Note. Ministry of Agriculture, Fisheries and Food, Torry Research Station.
- Johnston, W.A., Nicholson, F.J., Roger, A., and Stroud, G.D. (1994). Freezing and refrigerated storage in fisheries. Technical Report 340, FAO Fisheries.
- Muhieddine, M., Canot, É., and March, R. (2008). Various approaches for solving problems in heat conduction with phase change. *International Journal of Finite Volume Method*, 6(1).
- Olver, P.J. (2014). *Introduction to Partial Differential Equations*. Undergraduate Texts in Mathematics. Springer.
- Pham, Q.T. (2006a). Mathematical modeling of freezing processes. In *Handbook of Frozen Food Processing and Packaging*, chapter 7. Taylor & Francis Group, LLC.
- Pham, Q.T. (2006b). Modelling heat and mass transfer in frozen foods: a review. *International Journal of Refrigeration*, 29, 876–888.

Appendix A. SIMULATION PARAMETERS AND APPROXIMATIONS FOR $k(T)$ AND $\kappa(T)$

T_{ref}	$[278.5 \ 278 \ 277.5 \ 277 \ 276.5 \ 276 \ 275.5 \ 275 \ 274.5 \ 274 \ 273.5 \ 273 \ 272.5 \ 273 \ 273.5 \ 274 \ 274.5 \ 275 \ 275.5 \ 276 \ 276.5 \ 277 \ 277.5 \ 278 \ 278.5]^T$ K
u_{ref}	\underline{u}
v_{ref}	0 K s^{-1}
T_{init}	$235 \cdot \mathbf{1}_{(25 \times 1)}$
u_{init}	\underline{u}
\underline{u}	283 K
\bar{u}	293 K
\underline{v}	-0.01 K s^{-1}
\bar{v}	0.01 K s^{-1}
\bar{T}	$285 \cdot \mathbf{1}_{(25 \times 1)}$
Q	$\mathbf{I}_{(25 \times 25)}$
R	10^{-2}
S	10^{-2}

$\mathbf{1}_{(n \times 1)}$ denotes a vector of ones with n elements.

$$k(T) = 7 \cdot 10^{-8} + 2.737 \cdot 10^{-7} \left[-\arctan \left(\left(\frac{T}{T_F - \Delta T} - 1 \right) 20000\pi \right) + \frac{\pi}{2} \right] + 4.35 \cdot 10^{-8} \left[\arctan \left(\left(\frac{T}{T_F + \Delta T} - 1 \right) 50000\pi \right) \right]$$

$$\kappa(T) = 1.543 \cdot 10^{-9} \left[-\arctan \left(\left(\frac{T}{T_F - \Delta T} - 1 \right) 50000\pi \right) \right] + 1.543 \cdot 10^{-9} \left[\arctan \left(\left(\frac{T}{T_F + \Delta T} - 1 \right) 50000\pi \right) \right]$$